Research Article

Cancer Prevention Research

Hepatic Premalignant Alterations Triggered by Human Nephrotoxin Aristolochic Acid I in Canines

Ke Jin[1], Kun-kai Su[2,3], Tong Li[1], Xia-qing Zhu[1], Qi Wang[1], Ren-shan Ge[4,5], Zong-fu Pan[1], Bo-wen Wu[1], Li-jun Ge[1], Yi-han Zhang[1], Yi-fan Wang[1], Guo-fang Shen[1], Dan-yan Zhu[1], Chun-sheng Xiang[2,3], Lan-juan Li[2,3], and Yi-jia Lou[1]

Abstract

Aristolochic acid I (AAI) existing in plant drugs from *Aristolochia* species is an environmental human carcinogen associated with urothelial cancer. Although gene association network analysis demonstrated gene expression profile changes in the liver of human *TP53* knock-in mice after acute AAI exposure, to date, whether AAI causes hepatic tumorigenesis is still not confirmed. Here, we show that hepatic premalignant alterations appeared in canines after a 10-day AAI oral administration (3 mg/kg/day). We observed c-Myc oncoprotein and oncofetal RNA-binding protein Lin28B overexpressions accompanied by cancer progenitor-like cell formation in the liver by AAI exposure. Meanwhile, we found that forkhead box O1 (FOXO1) was robustly phosphorylated, thereby shuttling into the cytoplasm of hepatocytes. Furthermore, utilizing microarray and qRT-PCR analysis, we confirmed that microRNA expression significantly dysregulated in the liver treated with AAI. Among them, we particularly focused on the members in let-7 miRNAs and miR-23a clusters, the downstream of c-Myc and IL6 receptor (IL6R) signaling pathway linking the premalignant alteration. Strikingly, when IL6 was added *in vitro*, IL6R/NF-κB signaling activation contributed to the increase of FOXO1 phosphorylation by the let-7b inhibitor. Therefore, it highlights the new insight into the interplay of the network in hepatic tumorigenesis by AAI exposure, and also suggests that anti-premalignant therapy may be crucial for preventing AAI-induced hepatocarcinogenesis. *Cancer Prev Res; 9(4); 324–34. ©2016 AACR.*

Introduction

Hepatocellular carcinoma (HCC) is one of the most lethal malignancies and the fourth most common cancer worldwide, with around 700,000 new cases each year (1,2). Environmental factors including dietary habits, lifestyle choices, and even drug therapeutics play important roles in most human cancers (3–5), including excessive alcohol consumption corresponding to HCC (6, 7). Plant drugs derived from *Aristolochia* spp. remain in use today for the treatments of snake bites, arthritis and gout, and coronary artery diseases (8,9), particularly in Asia and some other areas, with the potential for further exposure (10). *Aristolochia* herbs create a potential public health problem of considerable magnitude (11). Aristolochic acid (AA), an active mixture of AAI and AAII, existed in plant drugs from *Aristolochia* species. AAI, proven to be the cause of AA nephropathy in women, was associated with prolonged intake of Chinese herbal remedies containing AAI in dietary supplements for slimming for the first time in Belgium in 1991 (12). The patients had developed a high risk of upper tract urothelial carcinoma (about 50%) and, subsequently, bladder urothelial carcinoma (13,14). AAI can also induce tumors in multiple organs of mice within 56 weeks after the start of a 3-week treatment (15). Notably, NF-κB1 and c-Myc oncoprotein expression in kidney reach a peak at 12-day AAI administration of Hupki (human *TP53* knock-in) mice (16,17), suggesting a critical role of renal tumorigenesis in the short-term duration of AAI (16,17). Gene association network (GAN) analysis further suggests hepatocyte nuclear factor 4α gene (*Hnf4a*) and *Tp53* inhibition in AAI-treated Hupki mouse liver (DNA adduct nontarget; refs. 16,17). AA-like mutational signatures in 11 HCC genomes/exomes have also been reported (18). Transient inhibition of HNF4α initiates hepatocellular transformation through a microRNA (miRNA) inflammatory feedback loop circuit (19); however, whether short-term AAI exposure induces potential hepatocarcinogenesis is not confirmed so far.

Short-term AAI exposure markedly upregulates c-Myc oncoprotein expression in the kidney of Hupki mice (16). Overexpression of c-Myc can induce HCC with a high frequency in mice (20).

[1]Institute of Pharmacology and Toxicology, College of Pharmaceutical Sciences, Zhejiang University, Hangzhou, PR China. [2]State Key Laboratory for Diagnosis and Treatment of Infectious Diseases, Hangzhou, PR China. [3]Collaborative Innovation Center for Diagnosis and Treatment of Infectious Diseases, The 1st Affiliated Hospital, College of Medicine, Zhejiang University, Hangzhou, PR China. [4]The Population Council at the Rockefeller University, New York, USA. [5]Institute of Reproductive Biomedicine, the 2nd Affiliated Hospital, Wenzhou Medical University, Wenzhou, PR China.

Note: Supplementary data for this article are available at Cancer Prevention Research Online (http://cancerprevres.aacrjournals.org/).

K. Jin and K.-k. Su contributed equally to this article.

Corresponding Authors: Yi-jia Lou, Institute of Pharmacology and Toxicology, College of Pharmaceutical Sciences, Zhejiang University, 866 Yuhangtang Road, Hangzhou 310058, PR China. Phone: 86-571-88208403; Fax 86-571-88208402; E-mail: yijialou@zju.edu.cn; Lan-juan Li, The 1st Affiliated Hospital, College of Medicine, Zhejiang University, 79 Qingchun Road, Hangzhou 310003, PR China. E-mail: ljli@zju.edu.cn

doi: 10.1158/1940-6207.CAPR-15-0339

Activation of c-Myc oncogenic transcription factor (Myc) induces the oncofetal RNA-binding protein Lin28B expression in multiple human and mouse tumor models (21). The outcome subsequently inhibits the biogenesis of all let-7 miRNAs, thereby promoting embryo, stem cell, and tumor growth (22). In fact, up to 40% HCCs are clonal and thus are considered to originate from hepatic progenitor cells (HPC; refs. 23,24). Within human HCC, cells having signal transducers and activators of transcription 3 (STAT3), stemness factor Oct4 but lacking the TGFβ receptor type II (TBRII) and embryonic liver fodrin (ELF) are believed to be typical hepatic cancer progenitor-like cells (HCPLC; refs. 23,24). To date, however, whether the initial molecular events and signaling transduction are involved in the onset and progression of malignant HPCs is still not confirmed. Based on the fact that plant drugs derived from *Aristolochia* spp. remain in use even today, it is particularly important to explore the most relevant nodes of cross-talk and cooperativity of the signal molecules in the initial stage of HCPLC formation by AAI exposure.

MiRNAs, a kind of 20–23-nt noncoding functional RNA molecules, are critical downstream components of key oncogenic and tumor suppressor signaling pathways (25–27). Direct control of miRNA expression by oncogenic and tumor suppressor networks results in frequent dysregulation of miRNAs, which contributes to tumorigenesis (21). Short-term AAI exposure also causes NF-κB1 overexpression in the kidney of Hupki mice (16). In the immune system, enhanced regulation of NF-κB signaling is crucial for maintaining the normal function of immune cells and avoidance of tumorigenesis (28,29). Although the importance of miRNAs in the signal transduction of IL6 and NF-κB has been highlighted in human HCC (19,28,30) and in human acute-phase response of hepatocytes (31), to date, whether IL6R/NF-κB contributes to miRNA dysregulation, thereby causing premalignance in liver by short-term AAI exposure has not yet been illustrated.

In the present research, we found that c-Myc and Lin28B were overexpressed in the AAI-induced acute-phase hepatic pathological response in canines. Yet, AAI exposure enhanced the vulnerability of HPCs to HCPLCs. IL6R/NF-κB activation linking dysregulated miRNAs was involved in nodes of hepatic premalignant alteration. It sheds a new insight into the interplay of abnormal signaling activation in the AAI-induced premalignant process and suggests that anti-premalignant therapy may be an admissible strategy for preventing liver tumorigenesis caused by AAI exposure.

Materials and Methods

Animals and animal works

Ten-month-old male beagle canines were purchased from the ANNIMO Science and Technology Ltd [Certificate No. SCXK (Su) 2010-0002] and were maintained in a specific pathogen-free environment. The procedures for performing animal experiments were in accordance with the principles and guidelines of Zhejiang University for animal use. And a protocol was approved by the Institutional Animal Care and Use Committee of Zhejiang University, China (Ethics Code: No. zju2009108012Y).

AAI (purity >98%, HPLC, Delta) was mixed with filler and filled into capsules. Canines were randomly assigned to two groups (4 in each group) and given capsules with control filler or AAI filler (3 mg/kg/day, equivalent dose of mouse) for 10 days. Blood samples were collected at indicated days for serum alanine transaminase (ALT) and aspartate transaminase (AST) measurement. Canines were sacrificed 11 days after initiation of the treatment. Livers were excised immediately after sacrifice. Part of the liver was fixed in 4% (wt/vol) neutral buffered formalin (pH 7.4) and embedded in paraffin for histologic analyses; the remaining liver was immediately snap-frozen in liquid nitrogen and kept at −80°C until use.

Histologic evaluation

Liver sections were embedded in paraffin and prepared according to the protocol (16). Liver sections were stained with hematoxylin and eosin (H&E) to evaluate histologic damage. Immunohistochemical analysis was performed according to the protocol (2). Typically, mouse monoclonal antibody against STAT3 (Cell Signaling Technology, #9139, 1:600), rabbit monoclonal antibody against p-STAT3 (Tyr705, Cell Signaling Technology, #9145, 1:400), rabbit polyclonal antibody against p-FOXO1 (Ser256, Abcam, ab131339, 1:100), rabbit polyclonal antibody against Oct4 (Abcam, ab18976, 1:100), and rabbit polyclonal antibody against IL6Rα (Santa Cruz, sc-13947, 1:100) were incubated with liver sections respectively at 4°C overnight subsequently. The following staining were developed with an immunohistochemical staining kit (SA1022 or SA1021, Boster) and a DAB kit (AR1022, Boster) according to the instructions.

For immunofluorescent analysis, rabbit monoclonal antibody against c-Myc (Abcam, ab32072, 1:250), rabbit polyclonal antibody against Lin28B (Santa Cruz Biotechnology, sc-130802, 1:100), mouse monoclonal antibody against Oct4 (Abcam, ab59545, 1:1), rabbit monoclonal antibody against STAT3 (Cell Signaling Technology, #12640, 1:1000), rabbit polyclonal antibody against TBRII (Santa Cruz Biotechnology, sc-400, 1:100), rabbit polyclonal antibody against Oct4 (Abcam, ab18976, 1:100), mouse monoclonal antibody against ELF (344050, 1:100, Merck Millipore) were incubated with liver sections at 4°C overnight followed by incubation with Dylight 488 or 549–conjugated goat anti-mouse (GAM4882 or GAM5492, 1:500), goat anti-rabbit (GAR4882 or GAR5492, 1:500) secondary antibodies (Multisciences).

For TUNEL staining assays, liver sections were stained using an In Situ Cell Death Detection Kit (11684795910, Roche Diagnostics) following the manufacturer's instructions.

The samples were analyzed with a Leica phase-contrast microscope (DMI3000B) for immunohistochemical analysis and Olympus (BX61W1-FV1000) confocal microscope for immunofluorescent analysis. Digital images were analyzed using Leica Application Suite v4.2 and Olympus Fluoview FV1000, and figures were prepared by using Macromedia Fireworks v8.0.

Liver samples' molecular and biochemistry analysis

ELISA assays using the canine IL6 ELISA kit (CA6000; R&D Systems) were performed using the DTX 880 Multimode Detector (Beckman Coulter).

Western blot and coimmunoprecipitation analyses were performed according to the protocol (16). Briefly, liver tissues were homogenized with RIPA buffer. Nuclear and cytoplasmic proteins were separately isolated using a nuclear extraction kit (P0028, Beyotime). The following primary antibodies were used: Smad2/3 (#5678, 1:1,000), Smad4 (#9515, 1:1,000), p-IκBα (Ser32, #2859, 1:1,000), NF-κB p50 (#3035, 1:1,000), p65 (#4764, 1:2,000), c-Fos (#2250, 1:1,000), c-Jun (#9165, 1:1,000), EGFR (#4267, 1:1,000), p-EGFR (Tyr1068, #3777, 1:1,000), STAT3

(#12640, 1:1,000), p-STAT3 (Tyr705, #9145, 1:2,000), Janus kinase 2 (JAK2; #3230, 1:1,000), Akt (#9272, 1:1,000), p-Akt (Ser473, #4051, 1:1,000), and p-Akt (Thr308, #13038, 1:1,000; Cell Signaling Technology); Lin28B (sc-130802, 1:200), TBRII (sc-400, 1:200), p-Smad2/3 (Ser423/425, sc-11769, 1:200), IL6Rα (sc-13947, 1:200), and Lamin B (sc-365962, 1:100; Santa Cruz Biotechnology); Oct4 (ab18976, 1:500), TGFβ1 (ab64715, 1:250), p-TBRI (Ser165, ab112095, 1:200), c-Myc (ab32072, 1:10,000), FOXO1 (ab126826, 1:500), and p-FOXO1 (Ser256, ab131339, 1:500; Abcam, USA); GAPDH (Mab5465-040, Multisciences). Other information about primary antibodies used in Supplementary Fig. S1 is given in Supplementary Table S3. The HRP-conjugated secondary antibodies were goat anti-mouse (LK-GAM007), goat anti-rabbit (LK-GAR007), and rabbit anti-goat (LK-RAG007, Multisciences). Coimmunoprecipitation was performed for anti-STAT3 and Oct4 according to the protocol (32).

RT-PCR analysis

RT-PCR analysis was conducted according to the protocol (33). Briefly, total RNAs from liver tissues were isolated with Trizol reagent (Gibco BRL). The mRNA expression levels were normalized to the expression of the housekeeping gene *Gapdh*. The primer sequences and conditions are presented in Supplementary Table S1.

MiRNA microarray and target prediction

MiRNA microarray analysis was performed by KangChen Bio-tech (Shanghai) with Exiqon miRCURY LNA, which is available at GSE75474 (http://www.ncbi.nlm.nih.gov/geo/query/acc.cgi?acc=GSE75474). MiRNAs dysregulated >1.5-fold ($P<0.05$) in response to AAI were further evaluated using qRT-PCR by KangChen Bio-tech. MiRNA clusters were retrieved from miRBase (www.mirbase.org; ref. 34). Putative targets of miRNAs were predicted by the combination of TargetScan (www.targetscan.org) and miRDB (www.mirdb.org; refs. 35,36). Finally, the estimated target protein expression was confirmed by Western blot analysis.

Cell culture and miRNA transfection

The human HCC cell line HepG2 was purchased from the Shanghai Institute of Cell Bank, Chinese Academy of Sciences (purchase order number No. 22008), and the cell line was authenticated by passing the conventional tests of cell line quality control methods and the test of DNA profiling (STR). Cells were maintained in high glucose DMEM (12800-017, Life Technologies) supplemented with 10% fetal bovine serum (FBS; Gibco, Life Technologies). The cells were transfected with let-7b mimic or inhibitor, miR-27a mimic or inhibitor by Lipofectamine 2000 (11668-019, Invitrogen, Life Technologies), respectively, for 24 hours, then treated with or without IL6 (20 ng/mL, #200-06, PeproTech) for another 24 hours. Cells were collected after 48 hours. The sequences of miRNA mimic and inhibitor are shown in Supplementary Table S2.

Statistical analysis

Pairwise comparisons between continuous data were analyzed using an unpaired two-tailed Student *t* test, and multiple comparisons were analyzed by one-way ANOVA. All data were expressed as mean ± SD, and $P < 0.05$ were considered statistically significant. The bioinformatics data were analyzed by the Mann–Whitney *U* test, and $P < 0.05$ was considered statistically significant.

Results

AAI treatment causes liver injury related to apoptosis

As shown in Fig. 1A, AAI-treated liver sections displayed congestion with disorder structure and karyopyknosis. Meanwhile, TUNEL staining revealed an increased number of apoptotic cells ($P < 0.01$) in the liver section of AAI-treated canines (Fig. 1B). Serum ALT and AST levels showed time-dependent increases, indicating that liver functional damage was progressing. ALT levels were increased at day 5 and markedly elevated (by 20-fold, $P < 0.01$) at day 9 in the AAI-treated canines when compared with those of control. Similar results were observed for AST levels (Fig. 1C).

AAI treatment leads to c-Myc and Lin28B upregulation

In situ double-staining immunofluorescence exhibited the overexpression of c-Myc and Lin28B in the liver sections receiving AAI (Fig. 2A). Western blot analysis further showed that their expressions were upregulated by 2.5-fold in the AAI-treated liver compared with control ($P < 0.05$, Fig. 2B). In addition, the expression levels of HCC gene *α-Fetoprotein (Afp)* and AFP protein were increased and reached 10-fold or 5-fold higher than those in control, respectively ($P < 0.01$, Supplementary Fig. S1), implying that the liver might undergo premalignant lesion in response to AAI administration. These results revealed that short-term AAI exposure could lead to hepatic premalignant alterations in canines as early as orally administrated for 10 days.

AAI treatment induces HCPLC appearance

Here, we used the immunohistochemistry, Western blot, and coimmunoprecipitation assays to reveal the expression of Oct4 and its binding to STAT3 in the livers of canines receiving AAI. As a result, Oct4-positive cells emerged as clusters in response to AAI (Fig. 3A). Compared with negative control, the Oct4 protein level was significantly increased ($P < 0.01$, Fig. 3B), and bound to STAT3 in AAI-treated liver (Fig. 3C). Furthermore, *in situ* double-staining immunofluorescence demonstrated that some HPCs with the typical markers Oct4, STAT3, TBRII, and ELF appeared in liver sections by AAI exposure (Fig. 3D), implying that HPCs proliferated and migrated in response to AAI-induced apoptosis. Importantly, among them, a few cells co-labeled with Oct4 and STAT3, but lacking both TBRII and ELF, appeared in parallel (Fig. 3D), suggesting that premalignant alteration with a typical feature of HCPLCs formed in the liver receiving AAI. Considering that enhanced TGFβ signaling may promote development of HPCs (37), we further examined whether AAI treatment activated the TGFβ1/Smad pathway. As shown in Fig. 3E, the downstream events of TGFβ1, such as p-TBRI, p-Smad2/3 (including cytoplasm and nucleus), and Smad4, were phosphorylated or overexpressed. Unexpectedly, TGFβ1/Smad pathway activation did not affect the E-cadherin expression as reported (ref. 38 Supplementary Fig. S2).

AAI-induced hepatic miRNA dysregulation and related target validation

We next observed the dysregulated miRNAs and the related networks in the liver receiving AAI. The heat map represents

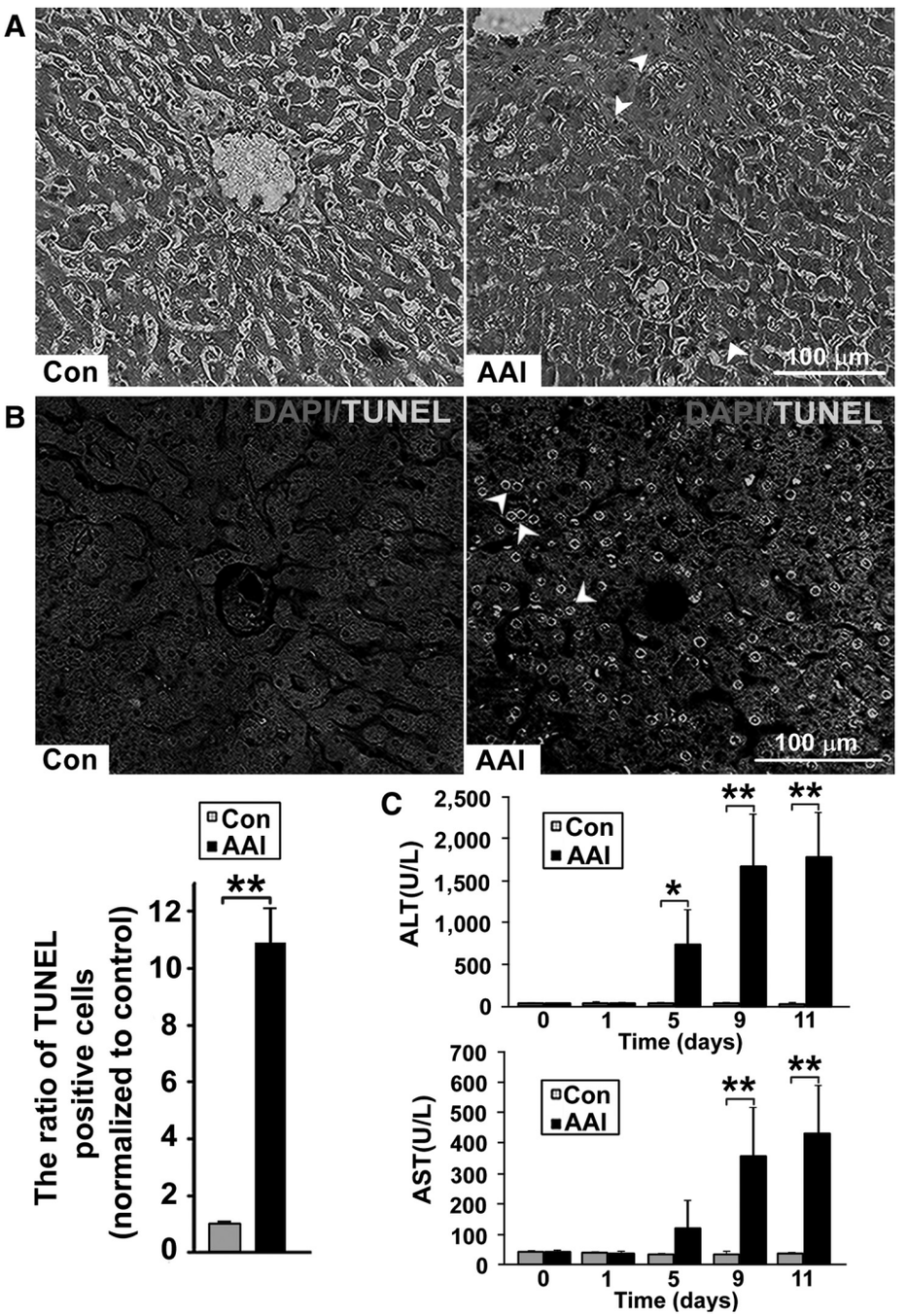

Figure 1.
Liver injury accompanied by apoptosis by AAI exposure in canines. A, H&E staining showed the lesion tissue (arrowheads); B, TUNEL staining displayed apoptotic cells (arrowheads) in liver sections from AAI-treated canines. The total number of apoptotic cells was normalized to the control in area of the tissue slice (cells/mm^2). C, elevated serum ALT and AST demonstrated liver functional damage in a time-dependent manner. Error bars, mean value ± SD; *, $P < 0.05$, **, $P < 0.01$ versus control. For each analysis, $n = 4$ per group.

miRNA microarray analysis of liver by AAI exposure compared with negative control (Supplementary Fig. S3). Especially, 10 miRNAs were predominantly differentially expressed and identified in liver by AAI exposure compared with the liver in control ($P < 0.05$, $P < 0.01$, Fig. 4A and B). Among them, cfa-let-7a-1∼let-7b miRNAs in the 10q12.3 chromosome region and cfa-miR-27a∼miR-24 in the 20q13.2 chromosome region (Supplementary Fig. S4) were closely linked to tumorigenesis or premalignant lesion. The qRT-PCR assay further confirmed that let-7a-1 and let-7b were decreased by 3.3-fold and 2.0–fold, respectively ($P < 0.01$), whereas miR-27a was increased by 1.95-fold and miR-24 by 2.5-fold ($P < 0.01$, Fig. 4B). Given that dysregulated miRNAs possess the enhanced post-transcriptional regulation in their targets, we therefore evaluated the possible effects of AAI exposure on putative targets of let-7a-1∼let-7b or miR-27a∼miR-24 according to the putative target intersections between TargetScan and miRDB (Supplementary Fig. S4). Western blot results showed the validation results of putative potential targets mentioned above (Supplementary Fig. S2).

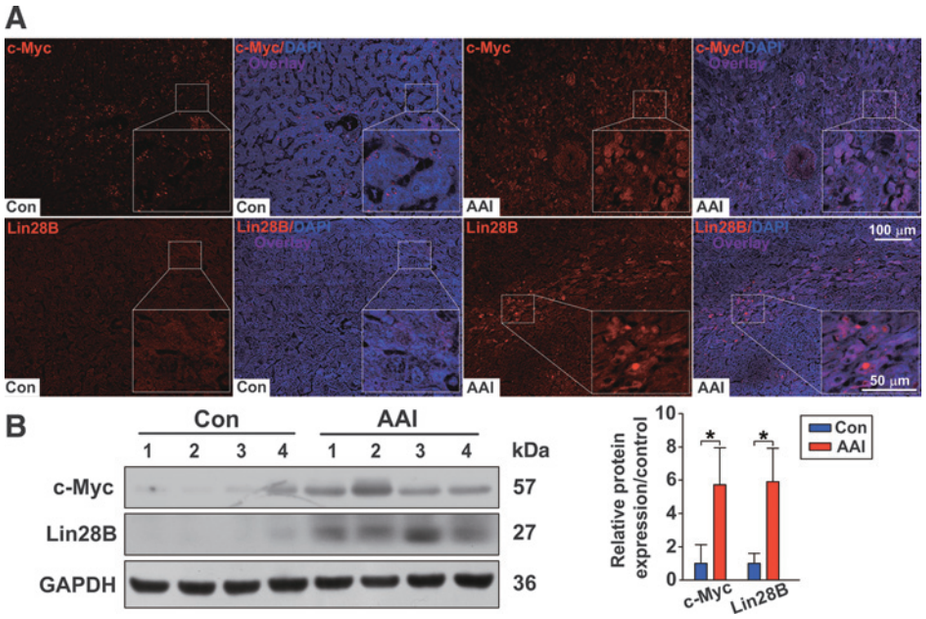

Figure 2.
AAI treatment increased c-Myc and Lin28B expression in liver. A, immunofluorescence staining demonstrated the c-Myc and Lin28B overexpression in the liver sections with AAI treatment. B, Western blot analysis showed that the c-Myc oncoprotein and its downstream event Lin28B were upregulated in the liver by AAI exposure. (More detailed information could be found in Supplementary Fig. S1.) Error bars, mean value ± SD; *, $P < 0.05$ versus control. For each analysis, $n = 4$ per group.

AAI exposure causes IL6R/NF-κB activation and FOXO1 phosphorylation

Lin28B is a negative regulator of let-7 miRNA, whereas let-7 could inhibit IL6R/NF-κB expression, forming a positive feedback loop connecting miRNA and its targets (28). Here, RT-PCR and ELISA assays demonstrated that *Il6* mRNA transcription and IL6 level in supernatant of AAI-treated liver were increased by 3-fold and 2.5-fold, respectively ($P < 0.05$, Fig. 5A and B). Western blot and immunochemistry analyses demonstrated that AAI treatment increased p-STAT3 expression by over 10 times ($P < 0.05$, Fig. 5C and D). Both IL6R and epidermal growth factor receptor (EGFR) activation can favor the STAT3 phosphorylation (p-STAT3). IL6R and its activator JAK2 protein levels were increased to 3-fold ($P < 0.05$) but not EGFR (Fig. 5D), suggesting that p-STAT3 was selectively triggered via IL6R activation in the liver by AAI exposure. We also found that the phosphorylated Akt (Ser473, Thr308) and phosphorylated IκBα were elevated in cytoplasm, while NF-κB (p50, p65) and activator protein (AP-1), c-Jun, were overexpressed in nuclei (Fig. 5E), indicating that IL6R/NF-κB signaling pathway activation promoted Lin28B/let-7 alteration in the liver by AAI exposure.

Immunohistochemical staining showed that hepatocytes had marginal nuclear FOXO1 staining and strongly positive cytoplasmic p-FOXO1 staining in response to AAI (Fig. 5F). Western blot analysis showed that FOXO1 in the nuclei was kept at a basal level, while p-FOXO1 in the cytoplasm was robustly increased by 22-fold compared with control ($P < 0.05$, Fig. 5G). It was the most significant alteration among all the targets of dysregulated miRNAs (Fig. 5, Supplementary Fig. S2).

Effects of IL6R/NF-κB activation on FOXO1/p-FOXO1 in let-7b or miR-27a oligonucleotide-transfected HepG2 cell line

The early hepatocarcinogenesis depends on paracrine IL6 production (39). We next further focused on the underlying roles of let-7b miRNA and miR-27a in the case of IL6 present *in vitro*. When incubated with IL6, let-7b inhibitor significantly upregulated Lin28B expression (Fig. 6A), indicating that let-7b oligonucleotide–transfected-HepG2 cell line kept the positive feedback loop that maintained the epigenetic transformed state as reported (28). To explore the possible mechanisms by which let-7b or miR-27a affected FOXO1 expression or its phosphorylation, the HepG2 cell line was incubated with IL6. As a result, let-7b inhibitor upregulated p-FOXO1 expression ($P < 0.05$, Fig. 6B), whereas miR-27a inhibitor promoted FOXO1 overexpression in an IL6-independent way ($P < 0.01$, $P < 0.05$, Fig. 6C). Notably, when IL6 was present, let-7b inhibitor and miR-27a mimic markedly increased p-STAT3 and NF-κB (p65) expression ($P < 0.05$, Fig. 6B and C), implying that miR-27a might be important to enhance IL6R/NF-κB signaling (Fig. 6D). These phenomena were quite similar to the signaling pathways observed in the AAI-treated canine liver.

Discussion

Plants containing AAI from *Aristolochia* species have been used for the treatment of arthritis and gout, as well as coronary artery diseases (8,9), also used for dietary supplements. Herbal drugs containing AAI can be nephrotoxic, genotoxic, and carcinogenic in humans, and AA is among the most potent 2% of carcinogens in the Carcinogenic Potency and Genotoxicity Databases (14,40). Although altered gene expression caused by AAI exposure is identified using GAN analysis in the liver of Hupki mice after a 3-week oral administration (16), to date, whether short-term duration of AAI can cause hepatocarcinogenesis is still poorly understood. Therefore, we chose beagle canine, a species with much closer biologic characteristics to human beings, as a suitable animal to explore the acute-phase cancerogenic mechanism in liver by AAI exposure. Considering that c-Myc oncoprotein expression reached a peak in AAI-treated kidney of Hupki mice at 12-day administration (16), here, we also explored the expression of c-Myc and its

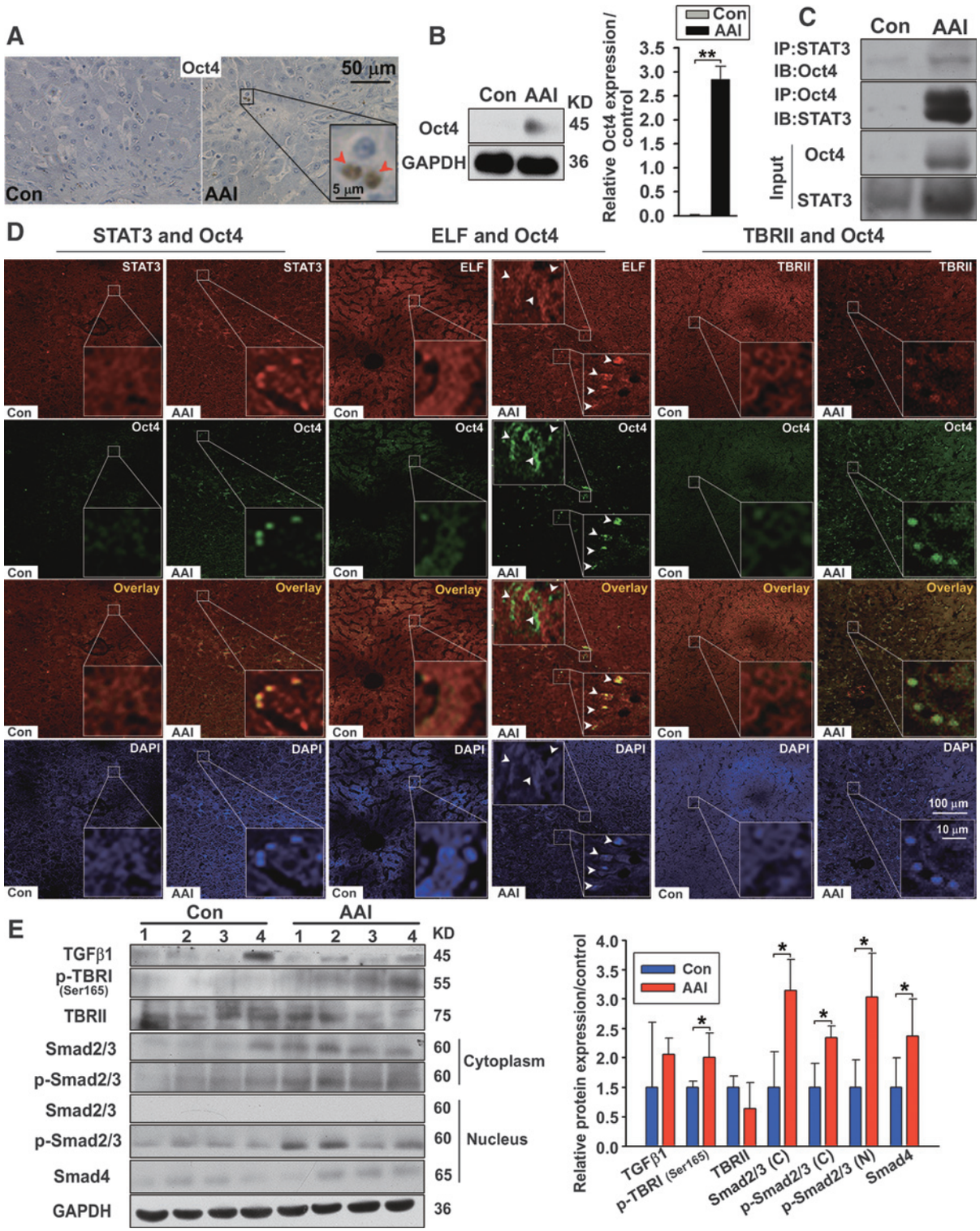

Figure 3.
AAI treatment induced HCPLC formation. A and B, immunohistochemistry and Western blot analysis displayed the increased Oct4-positive cells and upregulated Oct4 expression. C, coimmunoprecipitation showed that Oct4 binds to STAT3 in the liver section receiving AAI. D, immunofluorescence staining revealed the colocalization of Oct4 and STAT3 in the liver section receiving AAI (left, zoom), and a few Oct4-positive cells lost both ELF (upper left box in the middle panel, zoom) and TBRII expression (right, zoom). E, AAI treatment activated the TGFβ1/Smad pathway in the liver. Error bars, mean value ± SD; *, $P < 0.05$, **, $P < 0.01$ versus control. For each analysis, $n = 4$ per group.

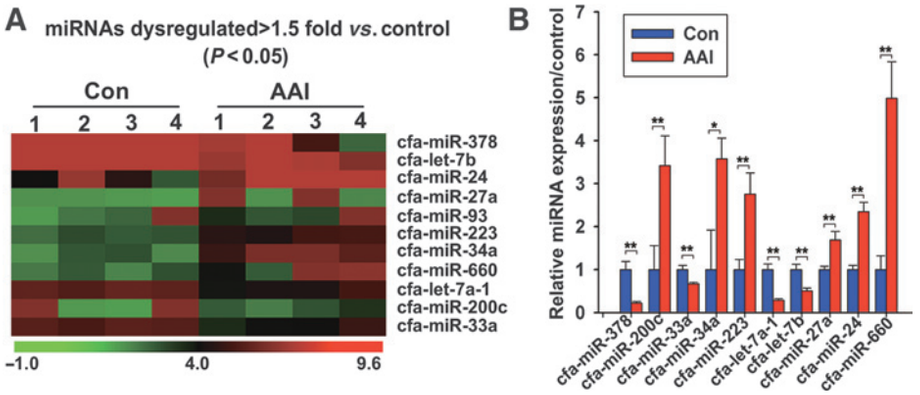

Figure 4.
Dysregulated miRNA expression and validation in the liver of canines by AAI exposure. A, heat map representing major changed miRNA microarray. B, qRT-PCR assay–validated 10 related miRNAs were predominantly expressed compared with control. Error bars, mean value ±SD; *, $P < 0.05$, **, $P < 0.01$ versus control. For each analysis, $n = 4$ per group.

downstream target Lin28B (41) in the 10-day AAI-treated canine liver. We found that the c-Myc and Lin28B were overexpressed in the AAI-induced acute-phase pathologic liver. Notably, for the first time, we found that HCPLCs appeared in the liver section, which was probably due to the acute AAI onset and progression of malignant HPCs. These findings confirmed that hepatic premalignant alterations did appear as early as in the short-term AAI exposure. The progression from normal cells to cancer is strongly influenced by environmental conditions and extracellular signaling pathways that affect the activity of tumor suppressors and oncoproteins (28). Our data imply that AAI-induced c-Myc and Lin28B overexpression might favor HCPLC formation. The liver injury induced by AAI was accompanied by apoptosis; we therefore suggested that HPCs would undergo proliferation, mobilization, and differentiation at the same time. Opposite to HCC tissue where impaired TGFβ signaling and activated IL6 signaling appeared together (2), our data revealed that AAI-induced acute-phase liver damage (apoptosis) resulted in TGFβ/Smads pathway activation, thereby promoting HPC proliferation, mobilization, and differentiation. The inconsistency between the levels of p-TBRI and nuclear p-Smad2/3 might result from the hepatic premalignance and regeneration, which makes the complexity of the TGFβ responses and which themselves may be regulated by a different signaling pathway (42).

Chemical carcinogenesis is a multistep process whereby cells acquire a series of genetic and epigenetic alterations in key growth-regulatory genes, such as oncogenes and tumor suppressors (16,17). Our results suggest that AAI-induced hepatic premalignant alterations might be associated with epigenetic disorders, thereby leading to c-Myc and Lin28B overexpression and HCPLC formation. We also confirmed that AAI oral administration resulted in some dysregulated miRNAs. Among them, functional members of let-7 miRNAs and miR-23a clusters, let-7a-1∼let-7b and miR-27a∼miR-24, closely linked to premalignance individually (19,21,28,41,43,44). The miRNAs in a cluster effectively cooperate by targeting the individual genes of the same pathway, thus justifying their coexistence (45,46). Clustered miRNAs jointly regulate proteins which lie in close proximity in the interaction network (45,46), and targeting these clustered miRNAs may provide a new perspective for the development of cancer chemoprevention (25). MiR-23a∼27a∼24 was directly induced by TGFβ in a Smad-dependent manner in human Huh-7 cells (44). In the present study, we further found that TGFβ signaling activated in the canine liver treated with AAI *in vivo*, which might take a double-response function, involved in both promoting HPC proliferation and migration (37) and upregulating miR-27a∼miR-24 expression (44). These results imply that in the case of TGFβ/Smad signaling pathway activation, upregulated miR-27a∼miR-24 may partially contribute to IL6R/NF-κB signaling, thereby promoting the vulnerability of HPCs to HCPLCs. The dysregulated miRNAs possess the enhanced post-transcriptional regulating effects on their targets. In the present study, we revealed the major effects of AAI exposure on putative targets of both the dysregulated miRNA clusters. Unexpectedly, TGFβ1/Smad pathway activation did not affect the E-cadherin expression as reported (38), indicating that the E-cadherin pathway was not involved in the AAI-induced hepatic premalignant alterations.

Lin28B is a negative regulator of let-7 miRNAs, while let-7 could inhibit IL6R/NF-κB expression (28). Our data indicate that IL6R/NF-κB (p50, p65) signaling activation promotes Lin28B/let-7 alteration in the liver by short-term AAI exposure, suggesting that the signaling transduction of c-Myc/Lin28B/let-7 coupled with IL6R/NF-κB contributes to AAI-induced acute premalignant transformation. Notably, in Hupki mice, 12-day AAI administration dramatically causes NF-κB (p50) rather than NF-κB (p65) overexpression in kidney (16). NF-κB can function as a tumor promoter in inflammation-associated cancer (28–30), but it is NF-κB (p65) that takes a role in regulating target gene transcription in nuclei; thus, our findings differ from the data in mice, and may be important in the development of AAI-associated hepatocarcinogenesis. The result implies that short-term AAI treatment triggers a strong immunologic and inflammatory response in the liver during the acute pathologic response phase, which subsequently contributes to the premalignant signaling cross-talk.

IL6R/STAT3/miR-24 has been defined as the component of an inflammatory feedback circuit regulating hepatocellular oncogenesis (19). Therefore, we focus only on the influence of AAI-induced IL6R/NF-κB signaling activation on FOXO1, a direct target of miR-27a (43), which has previously been linked to oncogenic transformation (47,48). The present study demonstrated that the p-FOXO1 level was robustly enhanced in liver by AAI exposure, and the hepatocytes with cytoplasmic p-FOXO1 were dramatically increased, while FOXO1 expression did not show significant changes. These results imply that in the case of c-Myc/

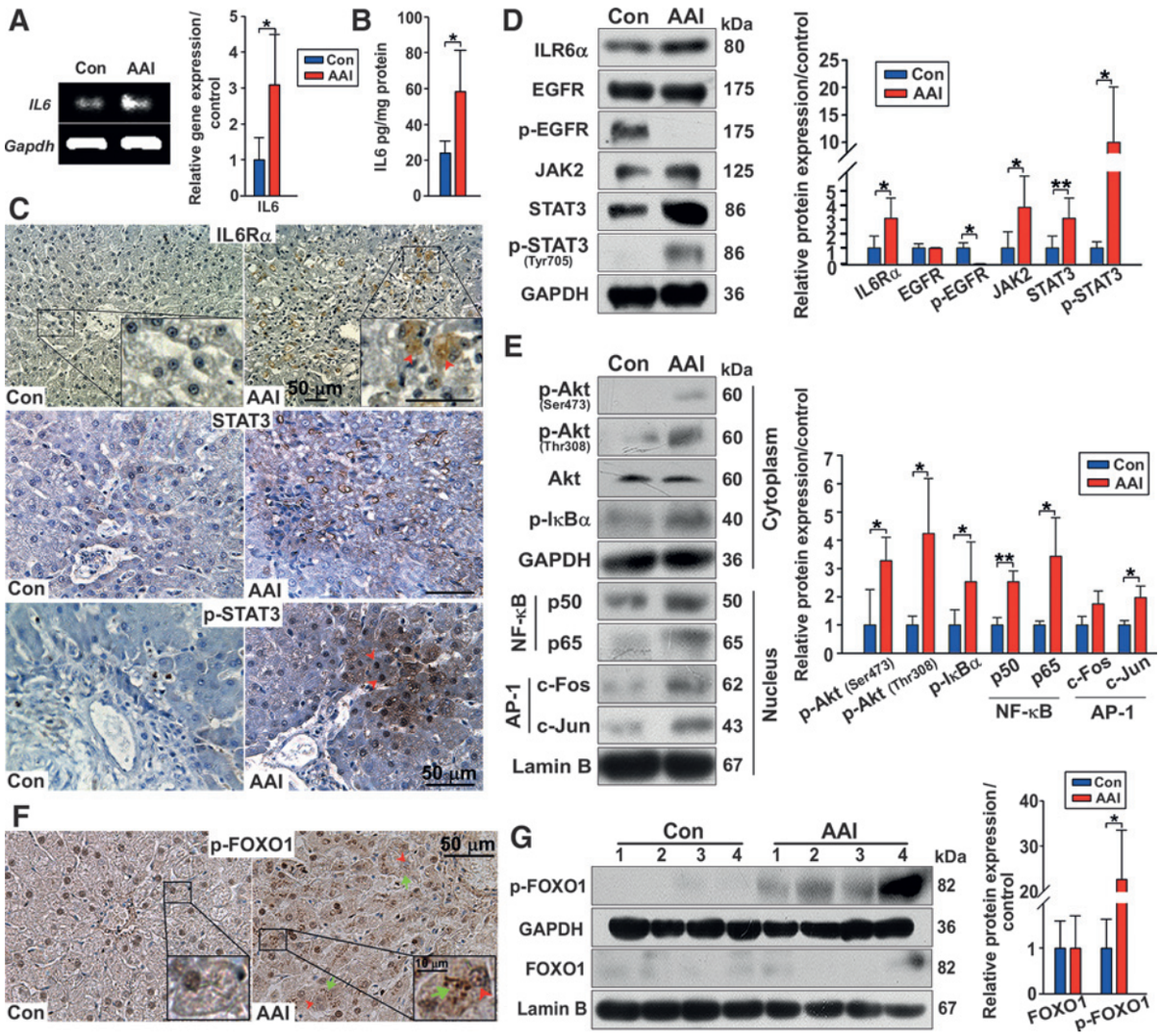

Figure 5.

Let-7 and miR-23a cluster target activation in the liver exposed to AAI. A and B, RT-PCR and ELISA assays demonstrated that *Il6* mRNA expression and supernatant IL6 level were increased in the liver receiving AAI. C and D, immunohistochemistry and Western blot showed IL6R/STAT3 was activated in liver sections by AAI exposure. E, the Akt/NF-κB pathway was activated in liver sections in response to AAI. F, immunohistochemistry showed the distribution of p-FOXO1 in nuclei (red arrow head) or in cytoplasm (green arrow). G, Western blot analysis showed that p-FOXO1 in the cytoplasm was robustly increased compared with control. Error bars, mean value ± SD; *, $P < 0.05$, **, $P < 0.01$ versus control. For each analysis, $n = 4$ per group.

Lin28B upregulation and IL6R/NF-κB signaling activation, FOXO1 phosphorylation and nuclear extrusion are increased through an unrevealed mechanism so far *in vivo*. Owing to its antiapoptotic nature (32), enhanced cytoplasmic p-FOXO1 may cause the premalignant cells to escape from apoptosis, including HCPLCs. The cells escaping from apoptosis may survive for a long time, and if HCPLCs happen to be among them, they will develop into HCCs.

It is well accepted that Akt and AP-1 transcription factors take part in the nuclear translocation and activation of NF-κB (28,49). Our *in vivo* results showed the Akt/NF-κB/c-Jun signaling activation, which could provide convincing support for the premalignant cross-talk from another side. Considering that the IL6R/STAT3 pathway is associated with NF-κB, c-Myc, and Lin28B expression (28), we further used the HepG2 cell line to investigate the IL6-induced acute-phase events. When IL6 was added *in vitro*, IL6R/NF-κB signaling pathway activation contributes to p-FOXO1 upregulation promoted by let-7b inhibitor, whereas miR-27a mimic might be important to enhance IL6R/NF-κB signaling. These results support the phenomenon appearing in our *in vivo* experiments, that is, the signaling transduction of c-Myc/Lin28B/let-7 coupled with IL6R/NF-κB contributes to AAI-induced acute premalignant transformation in the canine liver.

Our previous study revealed that compound compatibility in Guanxinsuhe, a compound preparation of *Radix Aristolochiea* (*Aristolochia debilis Sieb.* et Zucc) for treating coronary artery diseases, could affect the kinetic process of AAI and attenuate the

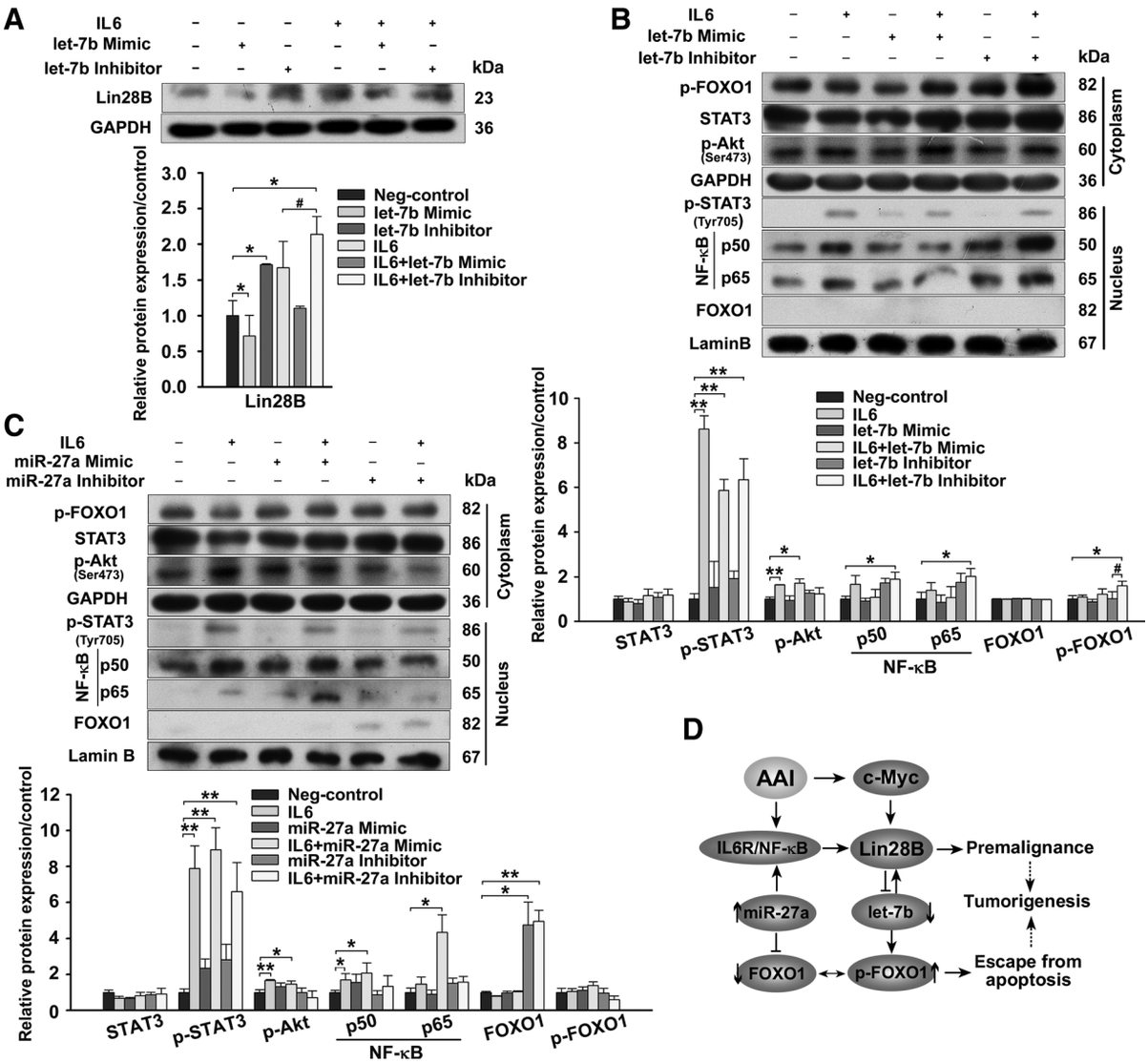

Figure 6.
The effects of IL6 on the let-7 or miR-27a oligonucleotide-transfected HepG2 cell line. A and B, in the case of IL6 present, let-7b inhibitor displayed enhanced effect on Lin28B, p-STAT3, NF-κB (p50, p65), and p-FOXO1 expression. C, in the case of IL6 present, miR-27a mimic promoted NF-κB (p50, p65) overexpression, whereas miR-27a inhibitor promoted FOXO1 expression. D, schematic representation of the functional co-contribution to hepatic premalignant alterations *in vivo* and *in vitro* (→: promoting effect, ⊥: inhibiting effect). Error bars, mean value ± SD; *, $P < 0.05$, **, $P < 0.01$ versus Neg-control; #, $P < 0.05$ versus IL6 present only. For each analysis, $n = 3$.

toxic effect on kidney in canines (50), indicating that intake of suitable dietary supplements probably is benefit for preventing AAI-induced liver injury. Our data further confirm the direct link between miRNAs dysregulation and IL6R/NF-κB signaling activation in liver in response to AAI. Therefore, targeting the network of the premalignant alterations could be a reasonable strategy for appropriating remedial measures against liver damage by AAI exposure.

Collectively, we find that let-7 miRNAs and miR-23a cluster dysregulation and IL6R/NF-κB signaling activation may synergistically contribute to c-Myc and Lin28B generation and probably enable the hepatic premalignant cells to escape from apoptosis in response to short-term AAI exposure. Therefore, it highlights the new insight into the interplay of the premalignant network in short-term AAI-exposed liver and suggests that anti-premalignant therapy may be an admissible strategy, thereby preventing liver from AAI-induced hepatocancerogenesis.

Disclosure of Potential Conflicts of Interest

No potential conflicts of interest were disclosed.

Authors' Contributions

Conception and design: Y.-J. Lou

Development of methodology: K. Jin, T. Li, Z.-F. Pan, B.-W. Wu, L.-J. Ge, Y.-H. Zhang, Y.-F. Wang, G.-F. Shen, C.-S. Xiang, Y.-J. Lou

Acquisition of data (provided animals, acquired and managed patients, provided facilities, etc.): K. Jin, T. Li, X.-Q. Zhu, Q. Wang, Z.-F. Pan, G.-F. Shen, Y.-J. Lou
Analysis and interpretation of data (e.g., statistical analysis, biostatistics, computational analysis): K. Jin, K.-K. Su, D.-Y. Zhu, L.-J. Li, Y.-J. Lou
Writing, review, and/or revision of the manuscript: R.-S. Ge, Y.-J. Lou
Administrative, technical, or material support (i.e., reporting or organizing data, constructing databases): K.-K. Su, X.-Q. Zhu, C.-S. Xiang, L.-J. Li, Y.-J. Lou
Study supervision: L.-J. Li, Y.-J. Lou
Other (bioinformatics analysis): K.-K. Su
Other (supervision of bioinfoamatics analysis): L.-J. Li

Grant Support

This work was supported by the National Natural Science Foundation of China (No 91229124 to Y.J. Lou, No 81401707 to K.K. Su), by the State Key Laboratory for Diagnosis and Treatment of Infectious Diseases (No 491010*A61203 to L.J. Li), and the Zhejiang Provincial Natural Science Foundation of China (No LZ12H31001 to Y.J. Lou).

The costs of publication of this article were defrayed in part by the payment of page charges. This article must therefore be hereby marked *advertisement* in accordance with 18 U.S.C. Section 1734 solely to indicate this fact.

Received September 16, 2015; revised December 8, 2015; accepted January 22, 2016; published OnlineFirst February 5, 2016.

References

1. Subramaniam A, Shanmugam MK, Perumal E, Li F, Nachiyappan A, Dai X, et al. Potential role of signal transducer and activator of transcription (STAT)3 signaling pathway in inflammation, survival, proliferation and invasion of hepatocellular carcinoma. Biochim Biophys Acta 2013;1835:46–60.
2. Tang Y, Kitisin K, Jogunoori W, Li C, Deng CX, Mueller SC, et al. Progenitor/stem cells give rise to liver cancer due to aberrant TGF-beta and IL-6 signaling. Proc Natl Acad Sci U S A 2008;105:2445–50.
3. Schmeiser HH, Stiborova M, Arlt VM. Chemical and molecular basis of the carcinogenicity of Aristolochia plants. Curr Opin Drug Discov Devel 2009;12:141–8.
4. Wild CP.Environmental exposure measurement in cancer epidemiology. Mutagenesis 2009;24:117–25.
5. Phillips DH.Polycyclic aromatic hydrocarbons in the diet. Mutat Res 1999;443:139–47.
6. Mercer KE, Hennings L, Sharma N, Lai K, Cleves MA, Wynne RA, et al. Alcohol consumption promotes diethylnitrosamine-induced hepatocarcinogenesis in male mice through activation of the Wnt/beta-catenin signaling pathway. Cancer Prev Res 2014;7:675–85.
7. Hassan MM, Hwang LY, Hatten CJ, Swaim M, Li D, Abbruzzese JL, et al. Risk factors for hepatocellular carcinoma: synergism of alcohol with viral hepatitis and diabetes mellitus. Hepatology 2002;36:1206–13.
8. Li L, Gao HM, Wang ZM, Wang WH. [Determination of aristolochic acid A in Guanxinsuhe preparations by RP-HPLC]. Zhongguo Zhong Yao Za Zhi 2006;31:122–4.
9. Vishwanath BS, Appu RA, Gowda TV. Interaction of phospholipase A2 from Vipera russelli venom with aristolochic acid: a circular dichroism study. Toxicon 1987;25:939–46.
10. Gokmen MR, Cosyns JP, Arlt VM, Stiborova M, Phillips DH, Schmeiser HH, et al. The epidemiology, diagnosis, and management of aristolochic acid nephropathy: a narrative review. Ann Intern Med 2013;158:469–77.
11. Grollman AP.Aristolochic acid nephropathy: Harbinger of a global iatrogenic disease. Environ Mol Mutagen 2013;54:1–7.
12. Debelle FD, Vanherweghem JL, Nortier JL. Aristolochic acid nephropathy: a worldwide problem. Kidney Int 2008;74:158–69.
13. Lemy A, Wissing KM, Rorive S, Zlotta A, Roumeguere T, Muniz MM, et al. Late onset of bladder urothelial carcinoma after kidney transplantation for end-stage aristolochic acid nephropathy: a case series with 15-year follow-up. Am J Kidney Dis 2008;51:471–7.
14. Nortier JL, Martinez MC, Schmeiser HH, Arlt VM, Bieler CA, Petein M, et al. Urothelial carcinoma associated with the use of a Chinese herb (Aristolochia fangchi). N Engl J Med 2000;342:1686–92.
15. Mengs U. Tumour induction in mice following exposure to aristolochic acid. Arch Toxicol 1988;61:504–5.
16. Arlt VM, Zuo J, Trenz K, Roufosse CA, Lord GM, Nortier JL, et al. Gene expression changes induced by the human carcinogen aristolochic acid I in renal and hepatic tissue of mice. Int J Cancer 2011;128:21–32.
17. Pozdzik AA, Salmon IJ, Husson CP, Decaestecker C, Rogier E, Bourgeade MF, et al. Patterns of interstitial inflammation during the evolution of renal injury in experimental aristolochic acid nephropathy. Nephrol Dial Transplant 2008;23:2480–91.
18. Poon SL, Pang ST, McPherson JR, Yu W, Huang KK, Guan P, et al. Genome-wide mutational signatures of aristolochic acid and its application as a screening tool. Sci Transl Med 2013;5:101r–197r.
19. Hatziapostolou M, Polytarchou C, Aggelidou E, Drakaki A, Poultsides GA, Jaeger SA, et al. An HNF4alpha-miRNA inflammatory feedback circuit regulates hepatocellular oncogenesis. Cell 2011;147:1233–47.
20. Simile MM, De Miglio MR, Muroni MR, Frau M, Asara G, Serra S, et al. Down-regulation of c-myc and Cyclin D1 genes by antisense oligodeoxy nucleotides inhibits the expression of E2F1 and in vitro growth of HepG2 and Morris 5123 liver cancer cells. Carcinogenesis 2004;25:333–41.
21. Chang TC, Zeitels LR, Hwang HW, Chivukula RR, Wentzel EA, Dews M, et al. Lin-28B transactivation is necessary for Myc-mediated let-7 repression and proliferation. Proc Natl Acad Sci U S A 2009;106:3384–9.
22. Nguyen LH, Robinton DA, Seligson MT, Wu L, Li L, Rakheja D, et al. Lin28b is sufficient to drive liver cancer and necessary for its maintenance in murine models. Cancer Cell 2014;26:248–61.
23. Mishra L, Banker T, Murray J, Byers S, Thenappan A, He AR, et al. Liver stem cells and hepatocellular carcinoma. Hepatology 2009;49:318–29.
24. Amin R, Mishra L. Liver stem cells and tgf-Beta in hepatic carcinogenesis. Gastrointest Cancer Res 2008;2:S27–30.
25. Yi B, Piazza GA, Su X, Xi Y. MicroRNA and cancer chemoprevention. Cancer Prev Res 2013;6:401–9.
26. He L, He X, Lowe SW, Hannon GJ. microRNAs join the p53 network–another piece in the tumour-suppression puzzle. Nat Rev Cancer 2007;7:819–22.
27. Mendell JT.miRiad roles for the miR-17–92 cluster in development and disease. Cell 2008;133:217–22.
28. Iliopoulos D, Hirsch HA, Struhl K. An epigenetic switch involving NF-kappaB, Lin28, Let-7 MicroRNA, and IL6 links inflammation to cell transformation. Cell 2009;139:693–706.
29. Pikarsky E, Porat RM, Stein I, Abramovitch R, Amit S, Kasem S, et al. NF-kappaB functions as a tumour promoter in inflammation-associated cancer. Nature 2004;431:461–6.
30. Ji J, Shi J, Budhu A, Yu Z, Forgues M, Roessler S, et al. MicroRNA expression, survival, and response to interferon in liver cancer. N Engl J Med 2009;361:1437–47.
31. Brock M, Trenkmann M, Gay RE, Gay S, Speich R, Huber LC. MicroRNA-18a enhances the interleukin-6-mediated production of the acute-phase proteins fibrinogen and haptoglobin in human hepatocytes. J Biol Chem 2011;286:40142–50.
32. Escribano C, Delgado-Martin C, Rodriguez-Fernandez JL. CCR7-dependent stimulation of survival in dendritic cells involves inhibition of GSK3beta. J Immunol 2009;183:6282–95.
33. Ogawa S, Tagawa Y, Kamiyoshi A, Suzuki A, Nakayama J, Hashikura Y, et al. Crucial roles of mesodermal cell lineages in a murine embryonic stem cell-derived in vitro liver organogenesis system. Stem Cells 2005;23:903–13.
34. Kozomara A, Griffiths-Jones S. miRBase: annotating high confidence microRNAs using deep sequencing data. Nucleic Acids Res 2014;42:D68–73.
35. Wong N, Wang X. miRDB: an online resource for microRNA target prediction and functional annotations. Nucleic Acids Res 2015;43:D146–52.
36. Agarwal V, Bell GW, Nam JW, Bartel DP. Predicting effective microRNA target sites in mammalian mRNAs. Elife 2015;4.
37. Mu X, Li Y. Conditional TGF-beta1 treatment increases stem cell-like cell population in myoblasts. J Cell Mol Med 2011;15:679–90.

38. Katuri V, Tang Y, Li C, Jogunoori W, Deng CX, Rashid A, et al. Critical interactions between TGF-beta signaling/ELF, and E-cadherin/beta-catenin mediated tumor suppression. Oncogene 2006;25:1871–86.
39. He G, Dhar D, Nakagawa H, Font-Burgada J, Ogata H, Jiang Y, et al. Identification of liver cancer progenitors whose malignant progression depends on autocrine IL-6 signaling. Cell 2013;155:384–96.
40. Some traditional herbal medicines, some mycotoxins, naphthalene and styrene. IARC Monogr Eval Carcinog Risks Hum 2002;82:1–556.
41. Wang Z, Lin S, Li JJ, Xu Z, Yao H, Zhu X, et al. MYC protein inhibits transcription of the microRNA cluster MC-let-7a-1∼let-7d via noncanonical E-box. J Biol Chem 2011;286:39703–14.
42. Yu JS, Ramasamy TS, Murphy N, Holt MK, Czapiewski R, Wei SK, et al. PI3K/mTORC2 regulates TGF-beta/Activin signalling by modulating Smad2/3 activity via linker phosphorylation. Nat Commun 2015;6:7212.
43. Guttilla IK, White BA. Coordinate regulation of FOXO1 by miR-27a, miR-96, and miR-182 in breast cancer cells. J Biol Chem 2009;284:23204–16.
44. Huang S, He X, Ding J, Liang L, Zhao Y, Zhang Z, et al. Upregulation of miR-23a approximately 27a approximately 24 decreases transforming growth factor-beta-induced tumor-suppressive activities in human hepatocellular carcinoma cells. Int J Cancer 2008;123:972–8.
45. Yuan X, Liu C, Yang P, He S, Liao Q, Kang S, et al. Clustered microRNAs' coordination in regulating protein-protein interaction network. BMC Syst Biol 2009;3:65.
46. Kim YK, Yu J, Han TS, Park SY, Namkoong B, Kim DH, et al. Functional links between clustered microRNAs: suppression of cell-cycle inhibitors by microRNA clusters in gastric cancer. Nucleic Acids Res 2009;37:1672–81.
47. Wang WS, Liu LX, Li GP, Chen Y, Li CY, Jin DY, et al. Combined serum CA19–9 and miR-27a-3p in peripheral blood mononuclear cells to diagnose pancreatic cancer. Cancer Prev Res 2013;6:331–8.
48. Melton C, Judson RL, Blelloch R. Opposing microRNA families regulate self-renewal in mouse embryonic stem cells. Nature 2010;463:621–6.
49. Song G, Ouyang G, Bao S. The activation of Akt/PKB signaling pathway and cell survival. J Cell Mol Med 2005;9:59–71.
50. Yang HY, Zheng XH, Du Y, Chen Z, Zhu DY, Lou YJ. Kinetics of aristolochic acid I after oral administration of Radix Aristolochiae or Guanxinsuhe preparation in canines. J Ethnopharmacol 2011;135:569–74.